

# Mannose 6-Phosphate/Insulin-like Growth Factor 2 Receptor Limits Cell Invasion by Controlling $\alpha V\beta 3$ Integrin Expression and Proteolytic Processing of Urokinase-type Plasminogen Activator Receptor

Herbert B. Schiller,\* Andreas Szekeres,\* Bernd R. Binder,<sup>†</sup> Hannes Stockinger,\* and Vladimir Leksa\*<sup>‡</sup>

\*Department of Molecular Immunology, Center for Physiology, Pathophysiology and Immunology, Medical University of Vienna, A-1090 Vienna, Austria; <sup>†</sup>Department of Vascular Biology and Thrombosis Research, Center for Biomolecular Medicine, Medical University of Vienna, A-1090 Vienna, Austria; and <sup>‡</sup>Institute of Molecular Biology, Slovak Academy of Sciences, 845 51 Bratislava, Slovak Republic

Submitted June 6, 2008; Revised October 27, 2008; Accepted November 18, 2008  
Monitoring Editor: M. Bishr Omary

The multifunctional mannose 6-phosphate/insulin-like growth factor 2 receptor (M6P/IGF2R) is considered a tumor suppressor. We report here that RNA interference with M6P/IGF2R expression in urokinase-type plasminogen activator (uPA)/urokinase-type plasminogen activator receptor (uPAR) expressing human cancer and endothelial cells resulted in increased pericellular plasminogen activation, cell adhesion, and higher invasive potential through matrigel. M6P/IGF2R silencing led also to the cell surface accumulation of urokinase and plasminogen and enhanced expression of  $\alpha V$  integrins. Genetic rescue experiments and inhibitor studies revealed that the enhanced plasminogen activation was due to a direct effect of M6P/IGF2R on uPAR, whereas increased cell adhesion to vitronectin was dependent on  $\alpha V$  integrin expression and not uPAR. Increased cell invasion of M6P/IGF2R knockdown cells was rescued by cosilencing both uPAR and  $\alpha V$  integrin. Furthermore, we found that M6P/IGF2R expression accelerates the cleavage of uPAR. M6P/IGF2R silencing resulted in an increased ratio of full-length uPAR to the truncated D2D3 fragment, incapable of binding most uPAR ligands. We conclude that M6P/IGF2R controls cell invasion by regulating  $\alpha V$  integrin expression and by accelerating uPAR cleavage, leading to the loss of the urokinase/vitronectin/integrin-binding site on uPAR.

## INTRODUCTION

The loss of the mannose 6-phosphate/insulin-like growth factor 2 receptor (M6P/IGF2R, CD222) has been described in many human malignancies, and it is considered a tumor suppressor (Scott and Firth, 2004; Hebert, 2006). M6P/IGF2R is a multifunctional receptor possessing distinct binding sites for structurally unrelated ligands and membrane partners (Ghosh *et al.*, 2003). It is not clear, however, what functional consequence of the loss of M6P/IGF2R is directly and determinedly responsible for tumor progression in vivo. First, the M6P/IGF2R-mediated degradation of insulin-like growth factor (IGF) 2 may play a role in suppression of tumor growth (Samani *et al.*, 2007). Second, the lack of M6P/IGF2R in tumor cells may also contribute to their

higher invasiveness due to impaired intracellular trafficking of cathepsins (Lorenzo *et al.*, 2000), observed also in M6P/IGF2R-deficient cell lines (Kasper *et al.*, 1996). Third, some of the M6P/IGF2R's ligands, such as retinoic acid and granzyme B, were shown to induce apoptosis via the receptor (Kang *et al.*, 1997; Motyka *et al.*, 2000). Fourth, the loss of M6P/IGF2R may reduce the availability of active transforming growth factor (TGF)- $\beta$  and thus its inhibitory effects on cell proliferation (Dennis and Rifkin, 1991; Godar *et al.*, 1999; Leksa *et al.*, 2005). Finally, M6P/IGF2R binds the urokinase-type plasminogen activator receptor (uPAR, CD87) and plasminogen (Plg), two components of the fibrinolytic system (Nykjaer *et al.*, 1998; Godar *et al.*, 1999; Leksa *et al.*, 2002; Kreiling *et al.*, 2003). Plg activation is crucial to direct cell migration through tissue barriers. On binding to uPAR, pro-urokinase (pro-uPA) is proteolytically activated to urokinase-type plasminogen activator (uPA), and in turn uPA specifically activates cell-bound Plg to the serine protease plasmin. Plasmin facilitates cell migration through degradation of extracellular matrix components both directly and through the activation of matrix metalloproteinases (Ragno, 2006). Virtually all types of cancer engage the fibrinolytic system during tumor progression (Dano *et al.*, 2005). Accordingly, the cell-associated activity and expression of uPA and uPAR strongly correlate with bad prognosis in most cancers (Dass *et al.*, 2008). Furthermore, the fibrinolytic system on endothelial cells is needed for angiogenesis

This article was published online ahead of print in *MBC in Press* (<http://www.molbiolcell.org/cgi/doi/10.1091/mbc.E08-06-0569>) on November 26, 2008.

Address correspondence to: Vladimir Leksa ([vladimir.leksa@meduniwien.ac.at](mailto:vladimir.leksa@meduniwien.ac.at)).

Abbreviations used: IGF, insulin-like growth factor; M6P/IGF2R, mannose 6-phosphate/insulin-like growth factor 2 receptor; Plg, plasminogen; PAI, plasminogen activator inhibitor; shRNA, short hairpin RNA; TGF, transforming growth factor; uPA, urokinase-type plasminogen activator; uPAR, urokinase-type plasminogen activator receptor.

and is hijacked by tumors for vessel growth (Mazar *et al.*, 1999).

In this study, we addressed the question which of the above-mentioned molecular interactions of M6P/IGF2R might be involved in regulating cell invasion. Using RNA interference with M6P/IGF2R in human cancer and endothelial cell lines, we show that M6P/IGF2R interacts with full-length uPAR and accelerates the proteolytic cleavage of uPAR, thereby interfering with the Plg activation cascade and thus cell invasion. Furthermore, the M6P/IGF2R knock-down cells up-regulate  $\alpha$ V $\beta$ 3 integrin expression, which has been associated with enhanced cell motility and invasion (Felding-Habermann *et al.*, 2001). Therefore, control over the proteolytic capacity and  $\alpha$ V $\beta$ 3 integrin expression of cells feature a tumor-suppressive role for M6P/IGF2R to hinder the metastatic progression of cancer.

## MATERIALS AND METHODS

### Materials

Vitronectin, pro-uPA, uPA, Glu-Plg, and plasminogen activator inhibitor (PAI)-1, all of human origin, were products of Technoclone (Vienna, Austria). Anti-mouse alkaline-phosphatase conjugate, Polybrene, galardin, amiloride, pepstatin A, iodoacetic acid (IAA), E-64, elastase, aprotinin, crystal violet, Triton X-100,  $\alpha$ 2-antiplasmin, human epidermal growth factor (EGF), and tranexamic acid (TA) were from Sigma-Aldrich (Vienna, Austria). Nonidet P-40 and EZ-Link Sulfo-NHS-biotin were from Pierce Chemical (Rockford, IL). Plasmin and uPA-specific substrates S-2251 and S-2444 were from CoaChrom Diagnostica (Vienna, Austria). Bovine serum albumin (BSA) was a product of Behring (Marburg, Germany). Streptavidin-Sepharose high performance was from GE Healthcare (Uppsala, Sweden).

### Antibodies

The monoclonal antibodies (mAbs) MEM-238 and MEM-240 to M6P/IGF2R and MEM-101A to  $\beta$ 1 integrin were from Dr. Václav Hořejší (Institute of Molecular Genetics, Academy of Sciences of the Czech Republic, Prague, Czech Republic); the mAbs H2 and C8 to uPAR were provided by Dr. Ulrich Weidle (Roche Diagnostics, Division Pharma, Penzberg, Germany). The rabbit polyclonal antibody (Ab) Ab32815 to M6P/IGF2R and the anti-uPAR Ab Ab27423 were both from Abcam (Cambridge, United Kingdom). The mAbs 3931, 3932, and 3936 to uPAR were from American Diagnostica (Stamford, CT). The mAb MAB1953, the Alexa Fluor 488-conjugated MAB1976X, both to  $\alpha$ V $\beta$ 3 integrin; the mAb CBL536 to  $\alpha$ 4 integrin; the mAb AB1928 to  $\alpha$ 5 integrin; and the mAb CBL458 to  $\alpha$ 6 integrin were all from Millipore Bioscience Research Reagents (Temecula, CA). The mAb MA-49A0 to  $\alpha$ 1 integrin was from Endogen (Woburn, MA). Antibodies against pro-uPA/uPA (35scuPA and 8scuPA) were from Technoclone. Neutralizing antibodies against TGF $\beta$  isoforms (anti-TGF $\beta$ 1 [AF-101-NA], anti-TGF $\beta$ 2 [AB-112-NA], and anti-TGF $\beta$ 3 [AB-244-NA]) were from R&D Systems (Minneapolis, MN); the IGF2 neutralizing antibody SIF2 was from Millipore (Lake Placid, NY).

### Cell Culture

All cells with exception of human umbilical vein endothelial cells (HUVECs) were cultured in RPMI 1640 medium (Sigma-Aldrich, St. Louis, MO) supplemented with 100  $\mu$ g/ml penicillin, 100  $\mu$ g/ml streptomycin, 2 mM L-glutamine, and 10% heat-inactivated fetal calf serum (FCS) (PAA, Linz, Austria). All cells were grown in a humidified atmosphere at 37°C and 5% CO<sub>2</sub> and passaged twice a week using trypsin-EDTA solution. Both primary and immortalized HUVECs were cultured in M199 medium supplemented with growth factors, heparin, and 20% FCS. The human kidney epithelial tumor cell line TCL-598 has been characterized previously (Koshelnick *et al.*, 1997) and was a gift from the Novartis Research Institute (Vienna, Austria). The human melanoma cell line IGR37 was from P. Petzelbauer (Department of General Dermatology, Medical University of Vienna, Vienna, Austria). The OVMZ-6 cells (Lutz *et al.*, 2001) were a kind gift from V. Magdolen (Technical University of Munich, Munich, Germany). Immortalized M6P/IGF2R-negative mouse fibroblasts were a kind gift of E. Wagner (IMP, Vienna, Austria).

### HUVEC Immortalization

The second generation lentiviral vector plasmid pWPT-green fluorescent protein (GFP) was kindly provided by D. Trono (Ecole Polytechnique Fédérale de Lausanne School of Life Sciences, Lausanne, Switzerland). Human telomerase reverse transcriptase (hTERT)-cDNA was inserted into pWPT-GFP between BamHI and Sall. Lentiviral particles were generated as described previously (Naldini *et al.*, 1996). Viral supernatants were harvested 2, 3, and 4 d after transfection, filtered through a 0.45- $\mu$ m filter, and used fresh.

The infection of primary HUVECs with the viral particle containing supernatant was performed four times on four consecutive days in the presence of 8  $\mu$ g/ml Polybrene (Sigma-Aldrich). The resulting immortalized HUVECs were termed HUVEctert. To control the lineage identity of HUVEctert, we tested cells for their ability to form vessel-like structures in a matrigel assay and for the induction of E-selectin upon tumor necrosis factor (TNF) treatment. Both, the induction of E-selectin by TNF and the formation of tubes in matrigel were normal compared with low-passage primary HUVECs. Furthermore, we analyzed the expression levels of CD31, CD105, CD109, and von Willebrand factor in HUVEctert, which were also comparable with primary HUVECs.

### Immunoprecipitation and Immunoblotting Analysis

Cells ( $5 \times 10^7$ ) were lysed in lysis buffer (20 mM Tris-HCl, and 150 mM NaCl, pH 7.5) containing 1% NP-40 and a mixture of protease inhibitors (5  $\mu$ M aprotinin, 5  $\mu$ M leupeptin, 5  $\mu$ M pepstatin, and 1 mM phenylmethylsulfonyl fluoride [PMSF]; all from Sigma-Aldrich). The cell lysates were subjected to immunoprecipitation using specific mAbs coated on a 96-well Falcon plastic plate via a goat anti-mouse immunoglobulin G (IgG) antibody (Sigma-Aldrich). After 3 h at 4°C, the wells were washed, and the immunoprecipitates were analyzed by SDS-polyacrylamide gel electrophoresis (PAGE) followed by transfer to Immobilon polyvinylidene difluoride membranes (Millipore, Billerica, MA). The membranes were blocked using 4% nonfat milk and immunostained with a specific mAb. For visualization of proteins, the ECL system with the Lumi-Imager (Roche Diagnostics, Mannheim, Germany) or the Odyssey infrared imaging system (LI-COR Biosciences, Lincoln, NE) was used.

### Flow Cytometry

Cells were detached using 5 mM EDTA/phosphate-buffered saline (PBS). For surface staining, the cells were washed with PBS containing 1% BSA and then incubated for 30 min with specific mAbs on ice. For nonlabeled antibodies, the cells were washed again, and a second step staining was done with fluorescein isothiocyanate-conjugated F(ab')<sub>2</sub> anti-mouse IgG + IgM antibodies (An der Grub, Kaumberg, Austria). Before analysis, the cells were washed with PBS/1% BSA. Dead cells were excluded by staining with 7-amino-actinomycin D. For intracellular staining, the cells were washed with PBS and subsequently fixed for 15 min with 4% paraformaldehyde. Then, the fixed cells were permeabilized by incubation for 15 min in PBS/5% FCS and 0.1% saponin. The staining was done on ice in the permeabilization buffer. Finally, the cells were washed twice in the permeabilization buffer. Flow cytometry was performed on an LSR II flow cytometer (BD Biosciences, Erembodegem, Belgium). Data acquisition was executed with the FACSDiva software (BD Biosciences). Data analysis was accomplished with the FlowJo software (Tree Star, Ashland, OR).

### Real-Time Polymerase Chain Reaction (PCR)

RNA was extracted from cells with Tri Reagent (Sigma-Aldrich). Total RNA was then reverse transcribed into cDNA using the High Capacity RNA-to-cDNA Kit (Applied Biosystems, Foster City, CA). Finally, gene expression was quantified by real-time PCR using a LightCycler instrument (Roche Diagnostics). The following primers were used: uPA, forward 5'-TGAGGTGGAAAACCTCATCC-3' and reverse, 5'-GGCAGGCAGATGGTCTGTAT-3'; uPAR, forward 5'-ACGACACCTTCCACTTCTG-3' and reverse, 5'-TCTCTCAGAGGAGCATCCA-3'; integrin  $\beta$ 1, forward 5'-TCTGCGGACAGTGTGTTGT-3' and reverse, 5'-CGTTGCTGCTTCAACAAGTA-3'; and integrin  $\beta$ 3, forward 5'-AGCTAGTCTGGGATCCACCTC-3' and reverse 5'-GGGGT-TAGTCTCGATGAAG-3'. Primers for integrins  $\alpha$ 4 and  $\alpha$ V and  $\beta$ 2-macroglobulin were described previously (Arap and Huang, 1999; Gruber *et al.*, 2003).

### RNA Interference

The stable knockdown cell lines for M6P/IGF2R were generated by the delivery of a short hairpin RNA (shRNA) expression cassette. We cloned three short hairpin sequences specific for M6P/IGF2R via EcoRI/AgeI to the lentiviral vector pLKOpurol (provided by S. Steward, Washington University School of Medicine, St. Louis, MO): 1) sh4525 with the sequence 5'-GAGCAACGACATGATGACTcaagagaGTCATCATGCTCGTTGCTC-3'; 2) sh5950 with the sequence 5'-GTTGTCTGCCCTCCAAAGAttcaagagaTCTTTGGAGGGCAGACAAC-3'; and 3) sh6588 with the sequence 5'-GCCCAACGATCAGCACTTctcaagagaGAAGTCTGATCGTTGGGC-3'. As a control construct, we used the MISSION nontarget shRNA control vector (pLKOpurol1) from Sigma-Aldrich. Lentiviral particles were generated as described previously (Naldini *et al.*, 1996). Briefly, human embryonic kidney (HEK)-293 cells were cotransfected by the calcium phosphate precipitation method with vector DNA (pLKOpurol1), the pseudotyping plasmid (pCMV\_VSV.G), and the packaging construct (pHR'8-2deltaR) in a ratio of 2:1:1.5. Forty-eight hours after transfection, viral supernatants were harvested, filtered, and used fresh for the transduction of target cell lines. The transduction was done overnight with the addition of 5  $\mu$ g/ml Polybrene. Transduced cell

lines were cultured permanently with puromycin (for TCL-598, 3  $\mu\text{g}/\text{ml}$ ; for HUVEctert, 2  $\mu\text{g}/\text{ml}$ ).

To silence the expression of uPAR and  $\alpha\text{V}$  integrin, we transiently transfected the TCL-598 cells using the Amaxa Nucleofector technology (Amaxa, Cologne, Germany). The following small interfering RNAs (siRNAs) were used: Silencer-validated siRNA targeting uPAR and the Silencer Negative Control siRNA were from Ambion (Austin, TX); Integrin  $\alpha\text{V}$  siRNA was from Santa Cruz Biotechnology (Santa Cruz, CA). TCL-598 cell transfection with 1  $\mu\text{g}$  of siRNA was optimized by testing various transfection programs on the Amaxa Nucleofector machine (Amaxa). The optimal transfection efficiency for TCL-598 cells was achieved with program B-24. We prepared the buffer for transfection as described previously (van den Hoff *et al.*, 1992). Assays were generally done 48 h after transfection.

### Plasmin and uPA Activity Assay

Plasmin and uPA activities were measured as described previously (Leksa *et al.*, 2002). Briefly, the TCL-598 ( $5 \times 10^4$  cells/well) or HUVEctert ( $1 \times 10^5$  cells/well) cells were seeded in 96-well plates 24 h before the assay. For the assay, the cells were washed twice with serum-free RPMI 1640 medium, and then they were incubated at 37°C in serum-free medium together with human Glu-Plg (50 nM) and either the chromogenic plasmin (S-2251) or uPA (S-2444) substrates. The absorbance change at 405 nm was monitored at different time points by using an enzyme-linked immunosorbent assay reader (SpectraMax M5; Molecular Devices, Sunnyvale, CA). To block the activity of unbound plasmin, the assays were performed in the presence of  $\alpha 2$ -antiplasmin (2.5  $\mu\text{g}/\text{ml}$ ). Optionally, various inhibitors were added to the reaction. In one set of Plg activation experiments the cells were preincubated with blocking antibodies (10  $\mu\text{g}/\text{ml}$ ) against IGF2 or TGF $\beta$  for 24 h before the assay. Also, during the assay time (4 h), the antibodies were present in the medium. The TGF $\beta$  blocking Abs were against all three isoforms of TGF $\beta$ .

### Cell Invasion Assay

Cell invasion was measured with the QCM Invasion assay kit according to the manufacturer's instructions (Millipore Bioscience Research Reagents). Briefly, the invasion assay is based on the Boyden chamber principle with filter inserts containing 8- $\mu\text{m}$  pore size polycarbonate membranes coated with basement membrane matrigel matrix. Optionally, the matrigel was preincubated with inhibitors diluted in serum-free medium for 1 h at 37°C. EGF was added into the lower chambers (10 ng/ml) in RPMI 1640 medium (10% FCS). Then, the cells were seeded into the upper part of the filter ( $1 \times 10^5$  cells/filter) and incubated 18 h at 37°C. The number of the cells invaded onto the lower side of the filters was evaluated after staining with crystal violet either by cell counting or by lysing the crystal violet stained cells followed by measuring the relative cell numbers on an enzyme-linked immunosorbent assay (ELISA) reader (OD595, SpectraMax M5; Molecular Devices).

### Cell Adhesion and Migration Assays

For cell adhesion and migration assays, the cells were harvested, washed, and resuspended in serum-free medium. For the adhesion assays, various matrix proteins were coated on a 96-well plate (Nalge Nunc International, Rochester, NY) in RPMI 1640 medium for 2 h at 37°C. Wells were blocked by using 1% BSA, washed, and then incubated with the cells ( $1 \times 10^5$  cells/well). After 10–20-min (TCL-598) or 60-min (OVMZ-6) incubation at 37°C, the wells were washed by immersion in a plastic tray containing PBS. Adhered cells were fixed with methanol and stained with crystal violet. After intense washings, cells were solubilized in 0.5% Triton X-100, and the number of cells was determined by measuring the absorbance at 595 nm using an ELISA reader.

Cell migration was measured in a modified Boyden chamber chemotaxis assay as described previously (Leksa *et al.*, 2002). Briefly, the cells ( $5 \times 10^4$ ) were seeded in the upper chambers of tissue culture polycarbonate filter inserts (10 mm in diameter, 8- $\mu\text{m}$  pore size; Corning Life Sciences, Lowell, MA) coated with vitronectin (10  $\mu\text{g}/\text{ml}$ ) and blocked with BSA. Chemoattractants (10 ng/ml EGF, 10 nM uPA, and 10  $\mu\text{g}/\text{ml}$  IGF2) were added to the lower chambers of the filter inserts. After 4–15 h of incubation at 37°C, the filters were removed, the upper surface of the membrane was scraped free of cells, and the number of cells that had migrated to the lower surface was measured by crystal violet as described above.

### Internalization and Biotin Chasing Assay

For the internalization assay, cells were harvested using 5 mM EDTA and washed with culture medium. Generally, the cells were put in suspension back to the incubator for at least 1 h after the EDTA treatment. Then, the cells were washed and stained on ice for 30 min with the uPAR mAb H2 conjugated with Alexa Fluor 488. After staining, the cells were washed with PBS and resuspended in 100  $\mu\text{l}$  of DMEM containing 1% BSA and 10 mM HEPES. Stained cells were incubated either on ice or for various times at 37°C to allow internalization. Afterward, the cells were stripped or not for 3 min in 0.5 M NaCl and 0.2 M acetic acid. The stripped cells were washed twice in DMEM with 1% BSA and 10 mM HEPES. Then, the remaining (stripping-resistant) fluorescence was analyzed by flow cytometry. The internalization rate was

calculated as a percentage of remaining fluorescence intensity after the stripping.

The biotin-chasing assay was done with either EDTA-detached or adherent cells that were washed with ice-cold PBS and cell surface biotinylated for 30 min on ice with 0.5  $\mu\text{g}/\text{ml}$  biotin. Incubation of the cells for 10 min with 100  $\mu\text{M}$  glycine in PBS stopped biotinylation. Then, the cells were washed two times and incubated in RPMI 1640 medium (10% FCS). Optionally, uPA, Plg, or the uPA inhibitor amiloride, a mixture of the serine protease inhibitors aprotinin and PMSF, or PAI-1 was added. After different times at 37°C, the incubation was stopped and the cells were lysed in radioimmunoprecipitation assay buffer. Then, the cell surface biotinylated proteins were precipitated with streptavidin beads for 2 h on 4°C. After washing the beads, the eluted precipitates were analyzed by SDS-PAGE and Western blotting. The bands on the immunoblot were quantified by analyzing the integrated intensity on the Odyssey infrared imaging system (LI-COR Biosciences). Values corresponding to full-length uPAR were normalized to  $\beta 1$  integrin bands. The normalized value at time 0 was set as 100%, and the percentage of degradation over time was calculated.

### Statistical Analysis

The experiments were performed at least two times in at least triplicates, and the data were expressed as mean values with SD. Statistical significance was evaluated using a two-tailed, paired Student's *t* test; a value of \**p* < 0.05 or \*\**p* < 0.005 (as indicated) was considered to be significant.

## RESULTS

### RNA Interference-mediated Silencing of M6P/IGF2R Increases Expression of uPAR and $\alpha\text{V}\beta 3$ , and Cell Surface Binding of uPA and Plg

To study the role of M6P/IGF2R in the fibrinolytic system of human tumor cells, we have chosen the human kidney carcinoma cell line TCL-598, because it expresses high amounts of both uPAR and its ligand pro-uPA (Koshelnick *et al.*, 1997). To perform loss of function studies, we used RNA interference to down-regulate M6P/IGF2R. TCL-598 cells were transduced with lentiviral constructs containing shRNA expression cassettes against M6P/IGF2R, leading to a stable silencing of the receptor. The most effective construct targeting M6P/IGF2R mRNA at the position 6588 resulted in a silencing efficiency of ~90% at the protein level and was used throughout the study (Supplemental Figure S1A and S1D). Another target position (sh4525) was almost equally efficient (~80% silencing efficiency), and importantly, we obtained similar results also with this target site (Supplemental Figure S1B, S1C, and S1E). Thus, we can exclude sequence-dependent nonspecific shRNA effects on the cells throughout our experiments. As a control, we used a scrambled nonspecific shRNA and in some experiments additionally the shRNA targeting position 5950 (sh5950), which did not repress M6P/IGF2R expression (Supplemental Figure S1).

Flow cytometry analysis revealed up-regulation of both surface and total pro-uPA/uPA in the M6P/IGF2R-silenced cells (24 and 35%; *n* = 3). We observed no change in the uPAR surface staining although the total protein amount was increased in the knockdown cells (38%; *n* = 3). Surface and total protein levels of  $\alpha\text{V}\beta 3$  integrin, which serves as alternative receptor for uPA (Tarui *et al.*, 2006), were also higher in knockdown cells (40 and 35%, respectively; *n* = 3) (Figure 1A). Other receptors such as  $\beta 1$  integrin or MHC class I remained unaffected.

We also observed an up-regulation of surface pro-uPA/uPA and  $\alpha\text{V}$  integrin in immortalized human umbilical vein endothelial cells (HUVEctert) silenced for M6P/IGF2R expression (48 and 39%, respectively; *n* = 2) (Figure 3A). In these cells, we observed a stronger up-regulation of  $\beta 1$  integrin expression (45%) than  $\beta 3$  (25%).

To test whether the up-regulation of uPA/uPAR and  $\alpha\text{V}\beta 3$  expression in TCL-598 cells was due to reduced protein turnover or enhanced mRNA levels, we quantified the

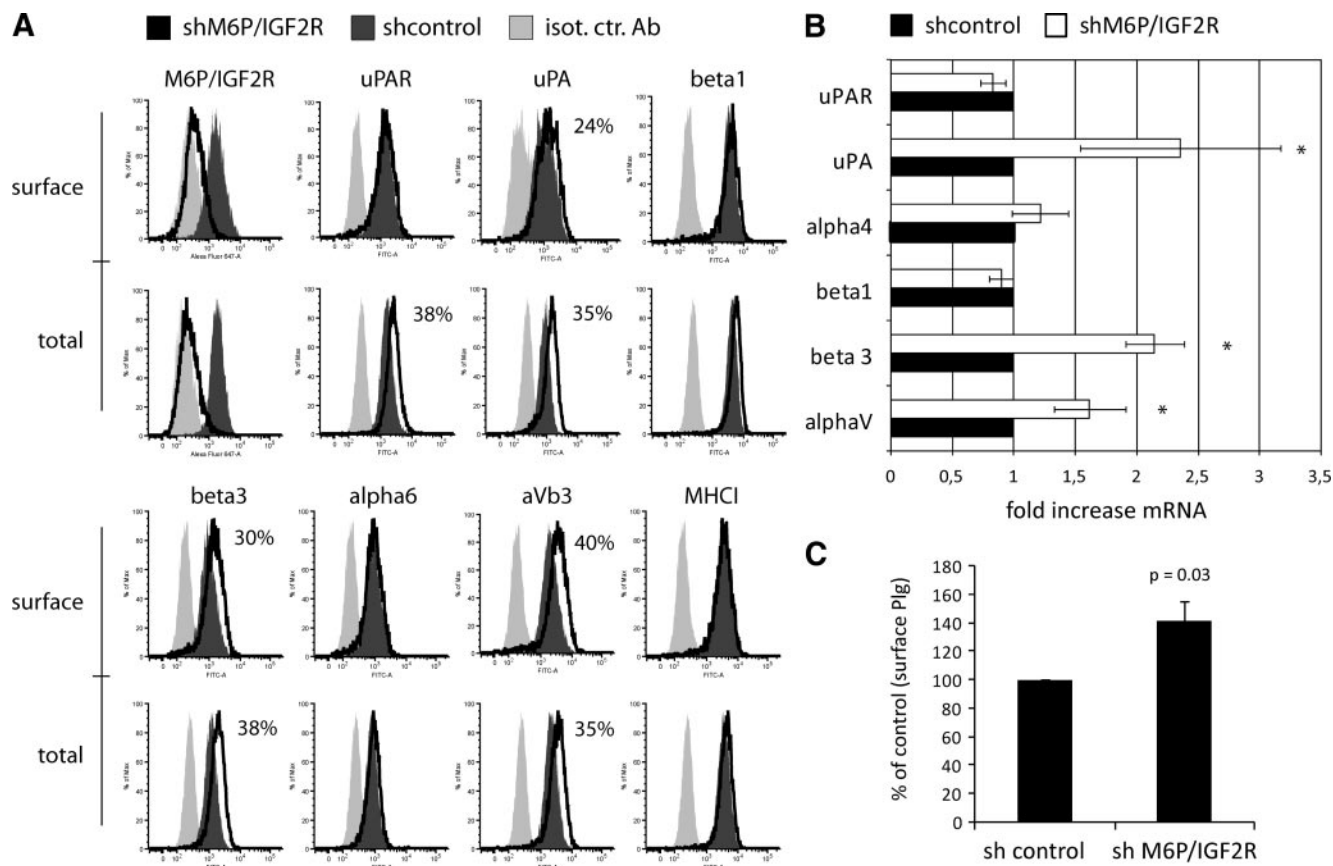


**Figure 1.** Increased expression of uPA/uPAR and  $\alpha V\beta 3$  and enhanced Plg binding upon M6P/IGF2R knockdown. (A) Surface and total expression of the indicated molecules in M6P/IGF2R silenced versus control shRNA transduced TCL-598 cells was analyzed by flow cytometry. The values show the percentage of up-regulated mean fluorescence intensity on M6P/IGF2R-silenced cells. Similar results were obtained in three other independent experiments. (B) The mRNA levels of the indicated molecules were analyzed using real-time PCR as described in *Materials and Methods*. The data represents three independent experiments (C) Cell surface binding of Cy5 labeled human Plg was analyzed by flow cytometry. Cy5-labeled BSA was used as a negative control. The bar graph shows the percentage of up-regulated mean Cy5 fluorescence intensity on M6P/IGF2R-silenced cells ( $n = 3$ ;  $p = 0.03$ ).

respective mRNAs by real-time PCR. The uPA and  $\alpha V\beta 3$  message was significantly higher in M6P/IGF2R knockdown cells, whereas  $\alpha 4$  and  $\beta 1$  mRNA were not affected (Figure 1B;  $n = 3$ ). Interestingly, also the uPAR mRNA was unchanged, although we found by flow cytometry the total protein amount in the silenced cells enhanced.

Because M6P/IGF2R, uPA as well as  $\alpha V\beta 3$  have been described as Plg receptors (Ellis *et al.*, 1999; Godar *et al.*, 1999; Tarui *et al.*, 2002), we tested next how the M6P/IGF2R knockdown changed the Plg binding capacity of the cells. We incubated the cells with Cy5-labeled Plg and analyzed the binding by flow cytometry. We found the Plg binding capacity to be higher by 35% on M6P/IGF2R-silenced cells (Figure 1C;  $n = 3$ ;  $p = 0.03$ ).

#### Enhanced Plasmin Activity and Invasion of M6P/IGF2R-silenced Cells Is Mediated by uPAR

Next, we measured the proteolytic activity of plasmin and uPA on the M6P/IGF2R knockdown TCL-598 cells. All assays were done in the presence of  $\alpha 2$ -antiplasmin (2.5  $\mu\text{g}/\text{ml}$ ), an inhibitor of unbound plasmin, to measure only the cell surface-associated proteolytic activity. The activity of both uPA and plasmin was significantly higher in the M6P/IGF2R knockdown cells (67 and 50% respectively;  $n = 3$ ; Figure 2, A and B, and Supplemental Figure S1). This en-

hanced proteolytic activity was sensitive to the lysine analogue TA (an inhibitor of the lysine-dependent binding of Plg onto the cell surface), the uPA inhibitor amiloride, and the serine protease inhibitor aprotinin. In contrast, the inhibitors of cysteine and aspartic acid proteases (IAA and pepstatin A) and matrix metalloproteinases (galardin) did not change the enhanced proteolytic activity of M6P/IGF2R knockdown cells (Figure 2, A and B). This excludes the possibility that either enhanced secretion or reduced internalization of cathepsin B, C, and L, which were shown to activate pro-uPA, was responsible for the observed phenotype. The enhanced cell surface plasmin activity on M6P/IGF2R knockdown cells was also not affected by blocking IGF2 and TGF $\beta$  (Figure 2C;  $n = 2$ ), excluding an autocrine IGF2 or TGF $\beta$  stimulation influencing the Plg activation system.

Of note, we detected enhanced cell surface plasmin activity (23%;  $n = 2$ ) also when M6P/IGF2R was silenced in either endothelial cells (Figure 3B) or the human melanoma cell line IGR37 (data not shown). This activity was as well independent of cysteine and aspartic acid proteases but dependent on uPA as evidenced by a rescue of the inhibitory phenotype with the addition of PAI-1, which blocks uPA-dependent Plg activation (Figure 3B).

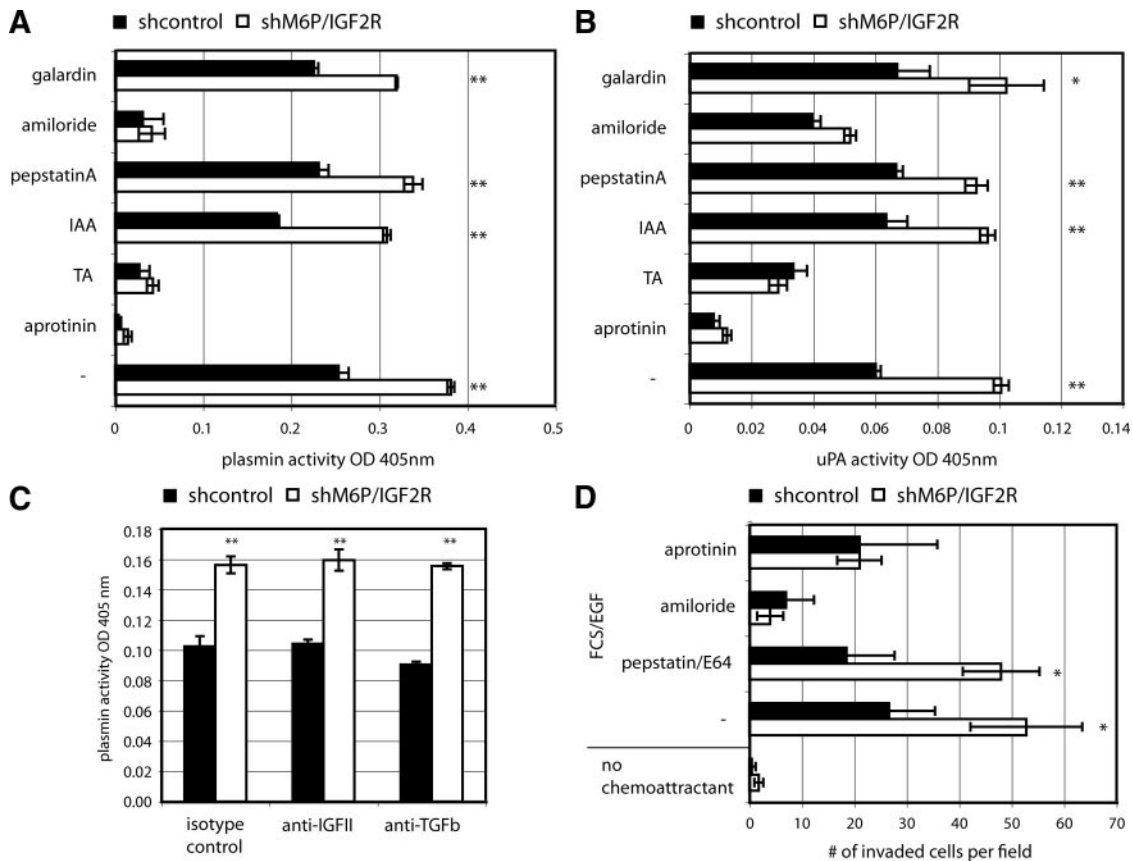


**Figure 2.** Enhanced cell surface uPA/plasmin activity and invasion of M6P/IGF2R knockdown cells. (A) Plasmin activity of M6P/IGF2R-silenced and control shRNA-transduced TCL-598 cells was analyzed by using the plasmin-specific chromogenic substrate S-2251. Plasmin activity was monitored at OD 405 nm by using an ELISA reader. The indicated inhibitors were added to the cells 20 min before adding Plg. (B) uPA activity was measured under the same conditions as in A by using the uPA-specific chromogenic substrate S-2444. (C) Cells were preincubated with the indicated blocking antibodies for 24 h, and plasmin activity was analyzed as described in A. Shown is a representative result of two independent experiments. (D) TCL-598 cells were analyzed in a Boyden chamber cell invasion assay using EGF (10 ng/ml) and FCS as chemoattractants. The concentrations of the used inhibitors: galardin (10  $\mu$ M), amiloride (10  $\mu$ M), pepstatin A (10  $\mu$ M), IAA (10  $\mu$ M), TA (5 mM), aprotinin (10  $\mu$ g/ml), and E-64 (10  $\mu$ M). Results are representative for two independent experiments.

Next, we tested TCL-598 cells in a cell invasion assay and found a 40% enhanced invasiveness of the M6P/IGF2R knockdown cells. The higher cell invasion in silenced cells was sensitive to uPA and serine protease inhibitors but not to cysteine and aspartic acid cathepsin inhibitors (Figure 2D;  $n = 2$ ).

The enhanced proteolysis and cell invasion observed in Figures 2 and 3 could be explained by the increased uPA/uPAR levels (Figures 1, A and B, and 3A) and/or the higher Plg binding capacity (Figure 1C) of the M6P/IGF2R knockdown cells. Furthermore,  $\alpha$ V $\beta$ 3 integrin, also up-regulated in these cells (Figure 1, A and B), was shown to bind both uPA and plasmin (Tarui *et al.*, 2002, 2006) and could thus be as well in charge. To test this, we generated double and triple knockdown TCL-598 cells (Figure 4A). First, we again tested the Plg activation capacity of the cells. The latter knockdown phenotype was completely rescued by cosilencing uPAR, whereas the  $\alpha$ V integrin/M6P/IGF2R double-silenced cells still held higher plasmin activity than the control cells (Figure 4B;  $n = 3$ ). Also in these experiments, plasmin activity was entirely sensitive to the uPA inhibitor amiloride. Next, we analyzed the contribution of uPAR and  $\alpha$ V integrins to the enhanced cell invasion in M6P/IGF2R knockdown cells. Both, uPAR and  $\alpha$ V cosilencing significantly rescued the enhanced cell invasion observed (Figure

4, C and D), indicating that also the enhanced  $\alpha$ V expression on M6P/IGF2R silenced cells contributed to the increase in cell invasion. Of note, we found a significant reduction of both uPA and Plg binding to the cell surface of uPAR-silenced cells but not to  $\alpha$ V-silenced cells (Supplemental Figure S2). These findings strongly suggest that M6P/IGF2R regulates pericellular Plg activation by acting directly on uPAR.

#### M6P/IGF2R Regulates Cell Adhesion and Motility

Apart from its role in extracellular matrix degradation, uPAR mediates cell adhesion and motility by binding directly vitronectin and regulating the activity of integrins (Madsen *et al.*, 2007; Madsen and Sidenius, 2008). In all cell lines in which we targeted M6P/IGF2R, we observed a marked increase in cell spreading under normal culture conditions. This could be attributed to the up-regulation of  $\alpha$ V integrins or a change in vitronectin binding to uPAR. To address this issue, we performed a cell adhesion assay on different matrix proteins. In addition to the TCL-598 cells that are very sticky and highly adhesive, we have chosen the OVMZ-6 ovarian carcinoma cell line, which possesses very low basal adhesiveness to most matrix proteins compared with TCL-598 cells. We silenced the expression of M6P/IGF2R in OVMZ-6 cells by shRNA expression as we did in

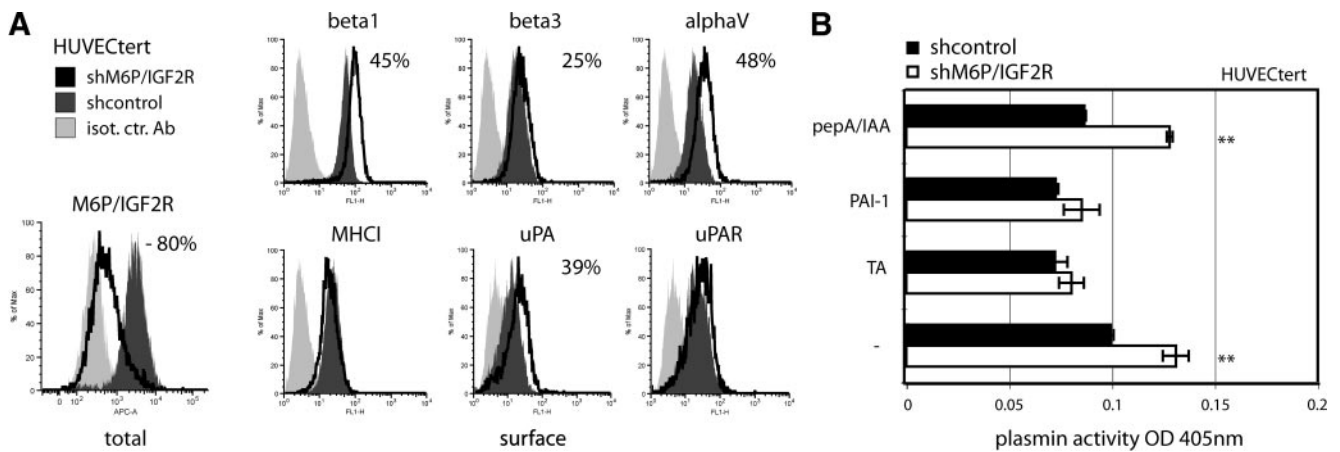


**Figure 3.** Enhanced uPA surface expression and plasmin activity in immortalized HUVECs silenced for M6P/IGF2R. HUVECs were immortalized by using telomerase reverse transcriptase (tert) and transduced with either M6P/IGF2R shRNA or control shRNA. (A) Surface and total expression of the indicated molecules was analyzed by flow cytometry. Histograms of a typical result are shown. The values indicate the percentage of altered mean fluorescence intensity of the M6P/IGF2R-silenced cells in comparison with the control cells. (B) Plasmin activity of M6P/IGF2R-silenced and control HUVECs was analyzed by using the plasmin specific chromogenic substrate S-2251. Plasmin activity was measured at OD 405 nm using an ELISA reader. PAI-1 was used at 10 U/ml. Other inhibitors were used as described in Figure 2. The shown data represent at least two independent experiments.

TCL-598 cells (Supplemental Figure S1D). M6P/IGF2R silenced OVMZ-6 as well as TCL-598 cells displayed significantly higher adhesiveness to vitronectin, fibronectin, and collagen type IV compared with control cells (Figure 5, A and C). Of these matrix proteins, only vitronectin is a ligand for uPAR; thus, these data indicated that rather the enhanced expression and/or activity of the  $\alpha V$  family integrin heterodimers was responsible for the increased cell adhesion of M6P/IGF2R knockdown cells. To confirm this assumption we again used double-silenced cells deficient for both M6P/IGF2R and uPAR or  $\alpha V$  integrins. Silencing of  $\alpha V$  resulted in loss of adhesion to vitronectin in control cells and in a significant reduction of the enhanced adhesion of M6P/IGF2R-silenced cells. We did not observe a complete rescue of the M6P/IGF2R knockdown phenotype, probably due to incomplete silencing of  $\alpha V$  integrin (Figure 5B). Interestingly, we did not see any effect of uPAR silencing on cell adhesion to vitronectin.

uPAR was recently shown to activate  $\alpha V\beta 3$  integrin and induce cell motility by activating Rac1 and Cdc42 (Wei *et al.*, 2008). To test whether M6P/IGF2R silencing also affected tumor cell motility, we subjected silenced TCL-598 and OVMZ-6 cells to a Boyden chamber chemotaxis assay and compared them with control cells. The Boyden chamber filters were precoated with vitronectin. TCL-598 cells showed very high basal migratory capacity (overnight transmigration 10–20% of total cells without any chemoattractant). For OVMZ-6 cells (no basal migration overnight), we used human pro-uPA, IGF2, and EGF as chemoattractants. Both OVMZ-6 and TCL-598 were found to significantly transmigrate with an enhanced rate upon M6P/IGF2R knockdown (Figure 5D).

#### *uPAR Cleavage but Not uPAR Internalization and Turnover Is Dependent on M6P/IGF2R Expression: M6P/IGF2R Accelerates uPAR Cleavage*

uPAR is present on the surface of cells as a full-length 3-domain molecule (D1D2D3), capable of binding pro-uPA/uPA, or a truncated variant (D2D3), lacking the pro-uPA/uPA binding domain D1. Coimmunoprecipitation analysis revealed that M6P/IGF2R interacted preferentially with the

intact full-length three-domain form of uPAR in TCL-598 cells (Figure 6A). In addition, we found M6P/IGF2R in a complex also with  $\alpha V$  integrin (Figure 6B).

Because we found both pro-uPA/uPA and uPAR up-regulated in the M6P/IGF2R knockdown cells, we tested whether the functional pro-uPA/uPA–uPAR complex was enriched in these cells. Indeed, the amount of uPAR coprecipitated with pro-uPA/uPA was higher (Figure 7A;  $n = 2$ ). Because we observed no change in surface uPAR (D1D2D3 + D2D3), measured by surface staining with an antibody against D2, on M6P/IGF2R-silenced TCL-598 cells (Figure 1B), we reasoned that surface expression of the full-length form must have been changed on these cells. To verify that, we biotinylated the cells, precipitated biotinylated surface proteins with streptavidin beads and visualized uPAR by SDS-PAGE and immunoblotting (Figure 7B). We found that in contrast to control cells, M6P/IGF2R knockdown cells expressed predominantly the full-length receptor (D1D2D3). The mean ratio of D1D2D3 to truncated D2D3 was 3.25 times higher in knockdown cells (Figure 7C;  $n = 5$ ;  $p = 0.02$ ). In these experiments, we again observed no significant difference in the abundance of cell surface uPAR (D1D2D3 + D2D3) between control and M6P/IGF2R-silenced cells (Figure 7D;  $n = 5$ ), which is in agreement with the flow cytometry analysis (Figure 1B).

Because M6P/IGF2R was proposed to be involved in the turnover of uPAR (Nykjaer *et al.*, 1998), it could have been possible that the abundance of full-length uPAR on the silenced cells was due to diminished internalization of the full-length uPAR enriching relative expression of the truncated D2D3 form. However, we did not find any significant defect in uPAR internalization rates upon M6P/IGF2R knockdown (Figure 8A;  $n = 4$ ).

It has been shown that uPAR can be cleaved by plasmin and uPA (Hoyer-Hansen *et al.*, 1992; Beaufort *et al.*, 2004). Because M6P/IGF2R binds both uPAR and Plg (Godar *et al.*, 1999; Leksa *et al.*, 2002), we asked whether M6P/IGF2R could influence the uPAR cleavage rate. Therefore, we chased the stability of cell surface uPAR on surface biotinylated TCL-598 cells for various times at 37°C. Afterward, the cells were lysed and biotinylated proteins were precipi-

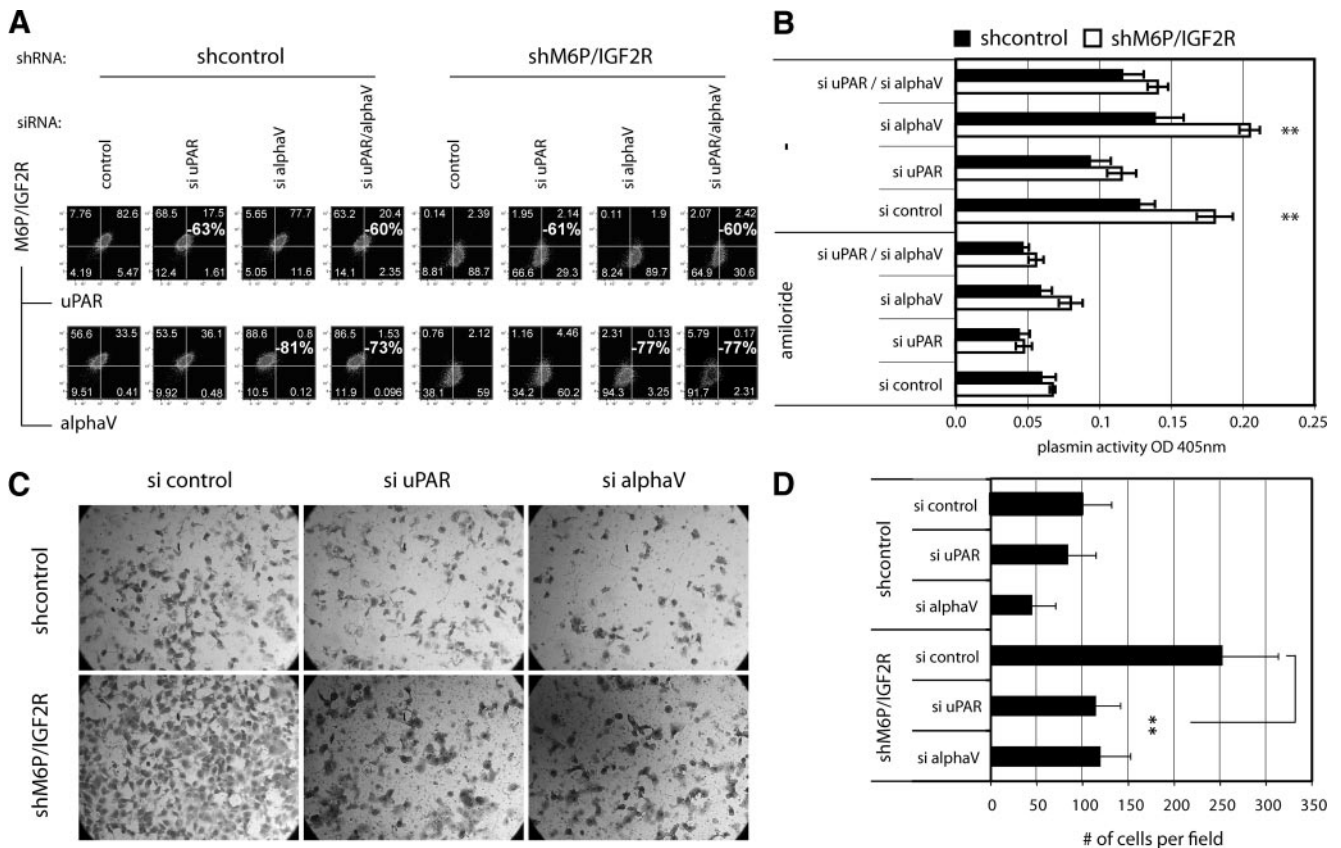


**Figure 4.** Genetic rescue of enhanced plasmin activity and cell invasion in M6P/IGF2R knockdown cells. (A) TCL-598 cells stably transduced with M6P/IGF2R shRNA or the control shRNA were transiently transfected with 1  $\mu$ g siRNA against uPAR,  $\alpha$ V integrin, or both. A scrambled nonspecific siRNA was used as control. Forty-eight hours after transfection, the cells were fixed, permeabilized, and analyzed for expression of the targeted molecules by flow cytometry. The values indicate the percentage of knockdown efficiency measured by the reduction of the mean fluorescence intensity. (B) Forty-eight hours after siRNA transfection, single, double, and triple knockdown cells were analyzed for cell surface plasmin activity as described in Figure 2A. (C) Alternatively the siRNA-transfected cells were seeded on a matrigel coated Boyden chamber, and cell invasion was analyzed as described in *Materials and Methods*. A representative phase contrast picture of crystal violet stained cells that have invaded through the matrigel is shown. (D) Two fields on three independent Boyden chamber filters of each specimen were evaluated for the number of invading cells. The mean number of cells per field is depicted ( $n = 2$ ).

itated with streptavidin. The precipitates were analyzed by SDS-PAGE and immunoblotting for occurrence of full-length uPAR (Figure 8B). We found that the stability of full-length uPAR (D1D2D3) was significantly enhanced in M6P/IGF2R-silenced cells at the onset of the experiment (within the first hour) (Figure 8C). This difference was due to reduced cleavage of uPAR in M6P/IGF2R knockdown cells, as shown by the sensitivity of the D1D2D3 stability to the uPA inhibitor amiloride (Figure 8C), aprotinin/PMSF and PAI1 (Supplemental Figure S2). At later times of the biotin chase experiment (4 h), we did not observe any difference in uPAR stability between control and M6P/IGF2R knockdown cells (Figure 8C). The bands corresponding to full-length uPAR were normalized to  $\beta$ 1 integrin, which was used as a loading control because we did not observe any M6P/IGF2R-dependent changes in the  $\beta$ 1 integrin turnover (Supplemental Figure S3A and S3C). In the same way, we analyzed also the turnover of  $\beta$ 3 integrin by chasing cell surface biotinylated integrins. The surface-biotinylated cell lysates were precipitated with streptavidin beads and the integrins were analyzed by Western blotting (Supplemental Figure S3B). By quantifying the biotinylated integrins, we could calculate the rate of degradation during the chasing experiment (Supplemental Figure S3D). The protein turnover rate of  $\beta$ 3

integrin was not changed upon M6P/IGF2R knockdown in TCL-598 cells.

To confirm the dependence of uPAR cleavage on M6P/IGF2R, we used mouse embryonic fibroblasts from M6P/IGF2R knockout mice transduced with human uPAR either alone or together with human M6P/IGF2R. The latter cells displayed significantly reduced Plg activatory capacity compared with the former cells (Leksa *et al.*, 2002). In contrast to TCL-598 cells, these cells do not produce human uPA. When biotinylated, both uPAR<sup>+</sup> and uPAR<sup>+</sup>/M6P/IGF2R<sup>+</sup> cells expressed predominantly the full-length variant of cell surface uPAR. When we performed the chasing experiments in the presence of active uPA, we found that surface biotinylated uPAR was rapidly cleaved, especially when M6P/IGF2R was coexpressed (Figure 8D;  $n = 3$ ). Similar to TCL-598 cells silenced for M6P/IGF2R expression, the mouse fibroblasts expressing human uPAR alone displayed significantly higher stability of the full-length D1D2D3 uPAR compared with the cells coexpressing human M6P/IGF2R (Figure 8E;  $n = 3$ ).

## DISCUSSION

Both the uPAR/Plg system and  $\alpha$ V $\beta$ 3 integrin are critically involved in tumor-associated angiogenesis and tumor

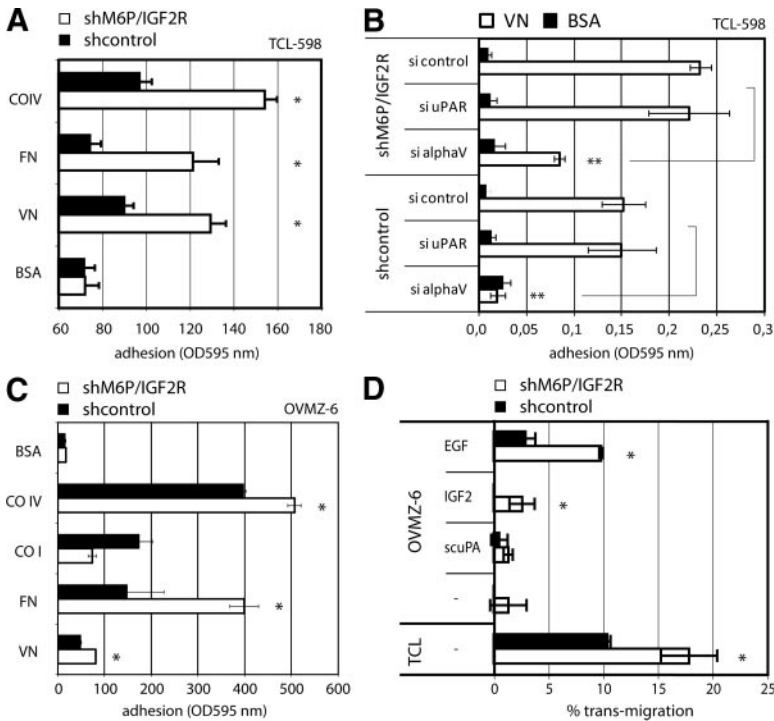


**Figure 5.** Enhanced cell adhesion and motility in M6P/IGF2R silenced cells. (A) Adhesion of TCL-598 cells on the indicated matrix proteins was determined as described in *Materials and Methods*. (B) Single and double knockdown cells characterized in Figure 4 were analyzed for their adhesion to vitronectin. (C) Ovarian carcinoma cells (OVMZ-6) transduced with M6P/IGF2R shRNA or control shRNA were analyzed for cell adhesion on the indicated matrix proteins. (D) Migration of OVMZ-6 and TCL-598 cells was tested in a Boyden chamber chemotaxis assay. EGF (10 ng/ml), IGF2 (10 ng/ml), or pro-uPA (10 nM) were used as chemoattractants. Adherent or transmigrated cells were fixed and stained with crystal violet. The stained cells were quantified at OD595 nm using an ELISA reader as described in *Materials and Methods*. VN, vitronectin; FN, fibronectin; COIV, collagen type IV; COI, collagen type I; BSA, bovine serum albumin.

spreading (Mazar *et al.*, 1999; Felding-Habermann *et al.*, 2001; Felding-Habermann *et al.*, 2002; Pilch *et al.*, 2002; Rolli *et al.*, 2003; Dano *et al.*, 2005; Dass *et al.*, 2008). Our results demonstrate that M6P/IGF2R functions as a negative regulator of the uPAR/Plg system and  $\alpha$ V integrin expression in human cancer and endothelial cells. First, the M6P/IGF2R interacts with full-length uPAR and facilitates its cleavage, thereby reducing the uPA/Plg binding capacity of cells. Second, the M6P/IGF2R knockdown induces up-regulation of the  $\alpha$ V integrins and cell adhesion to its ligands.

Consistent with the up-regulation of uPA and Plg binding to the cell surface, M6P/IGF2R knockdown cells exhibited enhanced pericellular plasmin activity and higher invasive capacity (Figures 1–3). As shown by the genetic rescue experiments using M6P/IGF2R-uPAR- $\alpha$ V double/triple knockdown cells (Figure 4), both the enhanced uPAR-mediated Plg activation and the enhanced  $\alpha$ V integrin expression contributed to an increase in cell invasion of M6P/IGF2R knockdown cells. Interestingly, silencing  $\alpha$ V $\beta$ 3 did not affect Plg activation, even though  $\alpha$ V $\beta$ 3 expression has been shown to enhance Plg activation on cells by binding both uPA and plasmin (Tarui *et al.*, 2002, 2006). Conversely, co-silencing either uPAR or  $\alpha$ V integrin in M6P/IGF2R-si-

lenced cells revealed that the enhanced adhesion to vitronectin was mediated by  $\alpha$ V integrin and not uPAR. A direct and strong function of uPAR in tumor cell adhesion to vitronectin is therefore not supported by our results, which is also in agreement with the findings of a recent report (Smith *et al.*, 2008).

Various cathepsins promote tumor invasiveness directly via degradation of extracellular matrix components or via activation of other proteinases, such as pro-uPA (Kobayashi *et al.*, 1991; Ravanko *et al.*, 2004). In addition, autocrine stimulation by IGF2 or TGF $\beta$  might influence the Plg activation system (Leivonen and Kahari, 2007; Samani *et al.*, 2007). Still, M6P/IGF2R-silenced cells held their phenotype compared with control cells in the presence of cathepsin inhibitors and IGF2/TGF $\beta$ -specific blocking antibodies (Figure 2). We therefore conclude that M6P/IGF2R regulates Plg activation and cell invasion via a direct effect on uPAR. The tumor cells used in our study produced high amounts of pro-uPA and expressed uPAR. In tumor cells producing low or no pro-uPA/uPAR, different suppressor functions of M6P/IGF2R could be decisive; for example, the lack of M6P/IGF2R could contribute to tumor cell invasiveness through impaired intracellular trafficking of cathepsins

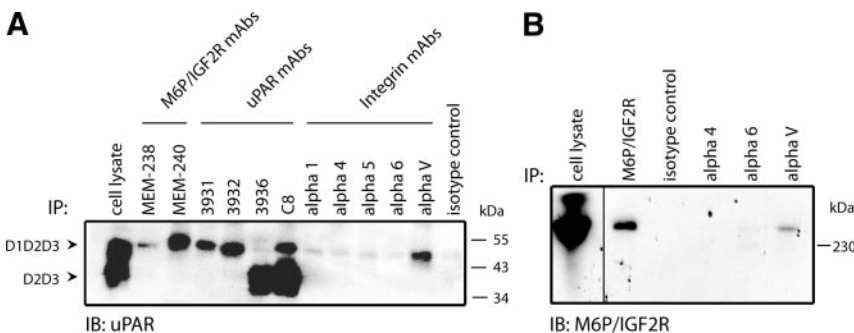


**Figure 6.** Coimmunoprecipitation of M6P/IGF2R, uPAR, and  $\alpha$ V integrin. (A) Lysates from TCL-598 kidney carcinoma cells were subjected to immunoprecipitation by using different mAbs as depicted against M6P/IGF2R, uPAR, and various integrin  $\alpha$  chains. The precipitates were analyzed by probing the Western blot with the uPAR mAb C8. (B) Some of the precipitates from A were also analyzed by immunoblotting with the polyclonal antibody Ab32815 against M6P/IGF2R.

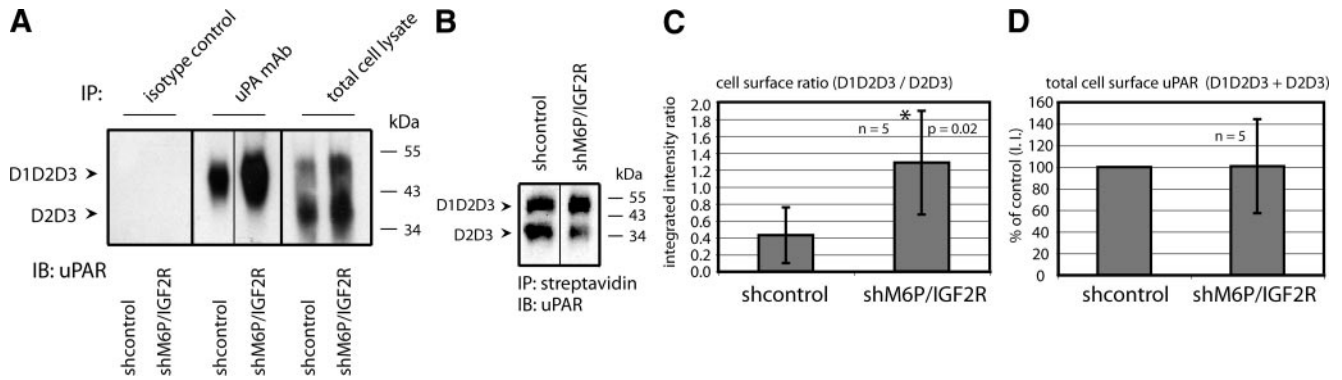


**Figure 7.** Dominance of full-length uPAR on the surface of M6P/IGF2R silenced cells. (A) uPA was precipitated from TCL-598 cell lysates by using the anti-uPA mAb. Coprecipitation of uPA and uPAR was compared in control and M6P/IGF2R knockdown cells by immunoblotting the precipitates with the anti-uPAR mAb C8. (B) Surface biotinylated cells were lysed and subjected to precipitation with streptavidin-coated Sepharose beads. Then, the precipitates were analyzed by immunoblotting with the polyclonal uPAR Ab. (C) The streptavidin precipitates from B were quantified by analyzing the integrated intensity (I.I.) of the uPAR bands on the immunoblot by using the Odyssey infrared imaging system (LI-COR Biosciences). The mean ratio of full-length uPAR to truncated D2D3 was calculated from five independent experiments ( $p = 0.02$ ;  $n = 5$ ). (D) Quantification of total surface uPAR (D1D2D3 + D2D3) in control and knockdown cells ( $n = 5$ ). The total expression of uPAR in the control cells was set as 100% I.I.

(Lorenzo *et al.*, 2000) or through degradation of IGF2 (MacDonald and Byrd, 2003; Guvakova, 2007).

In the coimmunoprecipitation experiments M6P/IGF2R had a strong preference to bind only full-length uPAR (Figure 6B). Similarly, just the intact full-length uPAR binds uPA (Behrendt *et al.*, 1991), vitronectin (Hoyer-Hansen *et al.*, 1997), and integrins (Montuori *et al.*, 2002). A coimmunoprecipitation of M6P/IGF2R only with full-length uPAR is in conflict with the findings of Nykjaer *et al.* (1998) who found also D2D3 interacting with M6P/IGF2R. This discrepancy could be due to the fact that in contrast to Nykjaer and colleagues, we did not use a chemical cross-linker before the immunoprecipitation. We cannot exclude a possible interaction of D2D3 with M6P/IGF2R; however, we propose that there is a preference for the full-length form. In vitro binding assays of truncated uPAR variants revealed that even domain 1 alone could bind to M6P/IGF2R. This interaction was strengthened by the presence of domain 2 and 3, suggesting that there might be multiple binding sites within the three different uPAR domains for M6P/IGF2R (data not shown).

In addition to the enhanced proteolytic capacity of M6P/IGF2R knockdown cells, the concomitant up-regulation of both uPA/uPAR and  $\alpha V\beta 3$  in these cells might feed a positive feedback loop leading to integrin activation. The binding of uPAR to the matrix protein vitronectin was proposed to feed integrin activation (Madsen *et al.*, 2007). Indeed, it has been recently shown that uPAR on podocytes activates  $\alpha V\beta 3$  in a vitronectin and lipid-dependent manner (Wei *et al.*, 2008). Furthermore, the engagement of  $\alpha V$  integrin by its ligand vitronectin led to induction of p38 and enhanced uPA expression in the invasive breast cancer cell line MDA-MB-231 (Chen *et al.*, 2001). The observed up-regulation of both  $\alpha V$  integrin and uPA/uPAR in the M6P/IGF2R knockdown cells suggest a molecular and functional overlap of uPA/uPAR, M6P/IGF2R, and  $\alpha V\beta 3$ . In this respect, it was also very interesting to find M6P/IGF2R coimmunoprecipitated with  $\alpha V\beta 3$  integrin (Figure 6). We did not find any binding of purified M6P/IGF2R to purified  $\alpha V\beta 3$  in vitro (data not shown), indicating that the interaction in cells is dependent on lipids and/or other third party molecules. Given that M6P/IGF2R is known for targeting some of its ligands to lysosomes, we analyzed the turnover rate of both  $\beta 1$  and  $\beta 3$

integrins; this was not changed upon M6P/IGF2R knockdown (Supplemental Figure S3). However, the level of  $\alpha V$  mRNA was enhanced in M6P/IGF2R silenced cells as determined by real-time PCR (Figure 1).

Two processes are described for internalization of uPAR: the first is dependent on a member of the LDL receptor family, such as the LDL-related protein and leads rather to reactivation instead of termination of uPAR functions during cell migration (Nykjaer *et al.*, 1997; Prager *et al.*, 2004). The second mechanism was proposed to be particularly dependent on M6P/IGF2R, targeting uPAR to lysosomes (Nykjaer *et al.*, 1998). This could be done either via direct internalization from the cell surface or sorting from endosomal compartments. Based on our data, the steady-state cell surface internalization rate of uPAR is not changed in M6P/IGF2R-silenced cells (Figure 8A). This could be explained by a sufficient redundancy with other internalization pathways. However, if M6P/IGF2R mediated the clearance of uPAR from the cell surface by internalization and transport to lysosomes, we would expect an enriched cell surface expression in M6P/IGF2R-silenced cells. We never observed altered surface expression of uPAR (D1D2D3 + D2D3) in M6P/IGF2R knockdown compared with control cells; instead, the ratio of full-length (D1D2D3) to truncated uPAR (D2D3) was changed (Figure 7). The function of M6P/IGF2R in lysosomal targeting of full-length uPAR cannot explain reduction of D2D3 in M6P/IGF2R knockdown cells.

As stated above, the TCL-598 tumor cell line used in this study secretes pro-uPA, and active uPA is known to cleave full-length uPAR on the surface of cells (Hoyer-Hansen *et al.*, 1992). In addition, plasmin can also cleave uPAR (Beaufort *et al.*, 2004). The cleavage of uPAR within the linker sequence of D1 and D2 was clearly shown to interfere with most of the uPAR functions (Montuori *et al.*, 2002, 2005); yet, under some circumstances the cleavage could also induce active processes such as the induction of chemotaxis via a G protein-coupled receptor (Resnati *et al.*, 2002) or the induction of myofibroblast differentiation (Bernstein *et al.*, 2007). Because uPA is a ligand for uPAR, and Plg can bind both M6P/IGF2R and uPA, the local accumulation of uPA and plasmin on the uPAR–M6P/IGF2R receptor complex might amplify the cleavage leading to loss of the uPA-binding site. In fact, a chasing assay revealed that M6P/IGF2R-silenced cells dis-

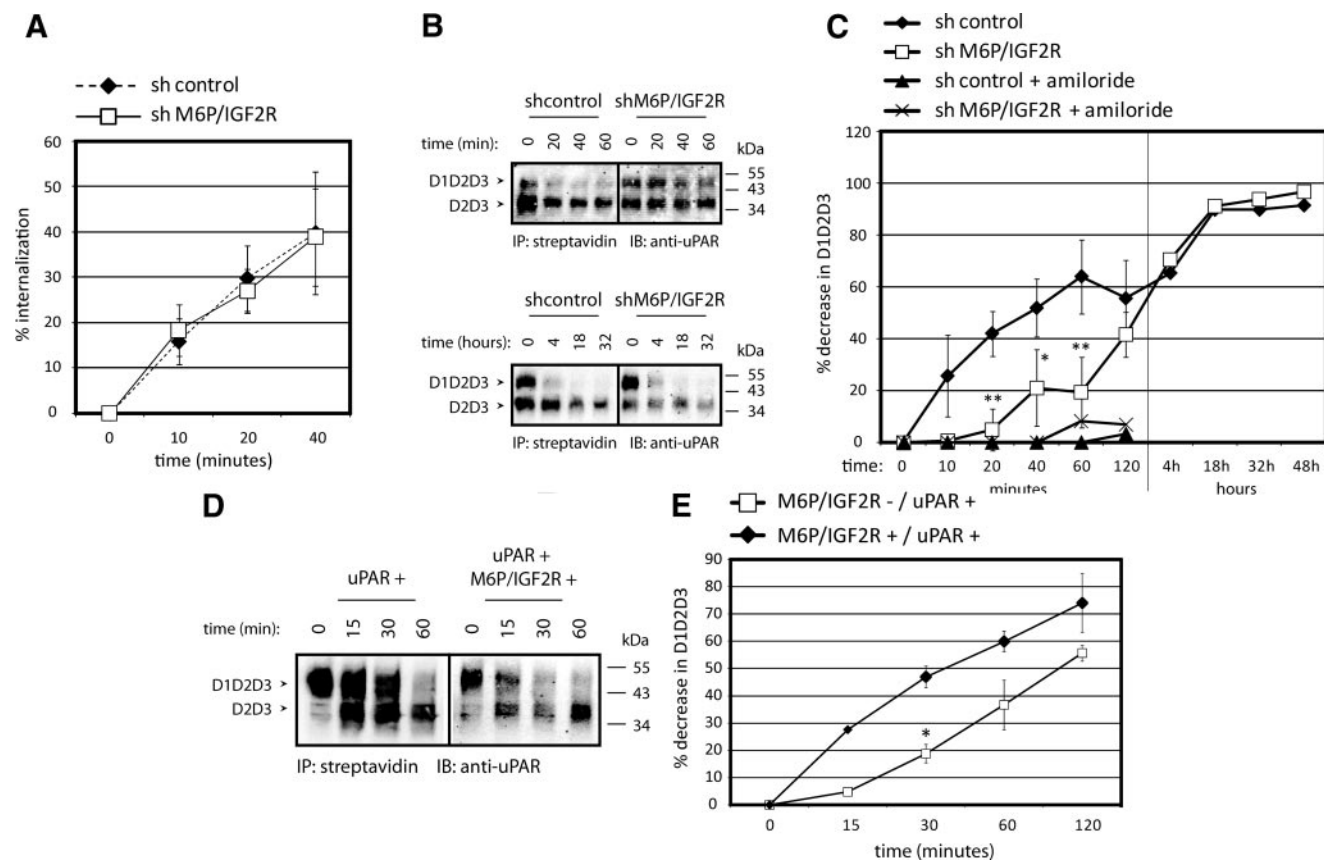


**Figure 8.** uPAR cleavage but not uPAR internalization and turnover is dependent on M6P/IGF2R expression. (A) TCL-598 cells were stained on ice with directly labeled anti-uPAR mAb H2. After incubation for the indicated times at 37°C, remaining cell surface mAbs were stripped with acid. Cells were analyzed for stripping-resistant (internalized) fluorescence by flow cytometry. Geometric mean values were calculated as percentage of internalized fluorescence ( $n = 4$ ). (B) Surface-biotinylated TCL-598 cells were incubated in culture medium supplemented with Plg (50 nM) for the indicated time points at 37°C. After incubation, the cells were lysed and biotinylated uPAR was analyzed by SDS-PAGE and immunoblotting. (C) Quantification of experiments shown in B; uPA activity was blocked by adding amiloride (10  $\mu$ M). The bands were quantified by analyzing the integrated intensity (I.I.) on the immunoblot using the Odyssey infrared imaging system (LI-COR Biosciences). The uPAR values were normalized for beta1 integrin and the percentage of decrease of full-length uPAR (D1D2D3) over time was calculated ( $n = 6$ ). (D) Surface-biotinylated M6P/IGF2R-negative mouse fibroblasts transduced with human uPAR and human M6P/IGF2R were incubated in culture medium supplemented with human uPA (10 nM) for the indicated times at 37°C. After incubation, the cells were lysed and biotinylated uPAR was analyzed as described in B. (E) Quantification of the integrated intensities of full-length uPAR (D1D2D3) normalized with an unspecific band on the immunoblot. The percentage of decrease of full-length uPAR (D1D2D3) over time was calculated ( $n = 3$ ).

play reduced cleavage of D1D2D3 to D2D3 at early time points (within 1 h) of the biotin chase (Figure 8). The cleavage was almost completely blocked by the uPA inhibitor amiloride, a mixture of the serine protease inhibitors aprotinin and PMSF, and partially blocked by addition of PAI-1 (Supplemental Figure S4), indicating that the cleavage is mediated or initiated by active uPA. uPAR seems to be more cleaved when dimerized within lipid rafts (Cunningham *et al.*, 2003) and complexed with integrins (Mazzieri *et al.*, 2006). To what extent these observations explain the role of M6P/IGF2R in uPAR cleavage needs future investigations. It might also be that the conformation of uPAR is changed by the interaction with M6P/IGF2R, thereby enhancing the cleavage rate. The fact that at later time points (starting at 2 h) of the biotin chase the initial difference in the cleavage kinetic is lost is very interesting. Cunningham *et al.* (2003) have shown that the half-life of uPAR (D1D2D3) upon addition of uPA to cells is only between 15 min (inside lipid rafts) and 1 h (outside lipid rafts). Exactly within this time frame we see a significantly slower decline in the level of biotinylated D1D2D3 in M6P/IGF2R knockdown cells (Fig-

ure 8C). Mouse fibroblasts overexpressing M6P/IGF2R showed the opposite phenotype (Figure 8E). This clearly indicates that the cell surface turnover of D1D2D3 by its cleavage is influenced by M6P/IGF2R expression.

After internalization, uPAR may be recycled back to the cell surface or degraded in lysosomes or by the proteasome. The later time points in Figure 8C (4–48 h) visualize that the turnover rate of biotinylated uPAR, which in addition to the cleavage of D1D2D3 to D2D3 also involves lysosomal and/or proteasomal degradation, is unchanged in M6P/IGF2R knockdown cells. These results are in divergence with a nonredundant function of M6P/IGF2R in mediating the lysosomal degradation of uPAR (Nykjaer *et al.*, 1998). In line with this, we also did not find a reduced accumulation of uPAR in lysosomes of M6P/IGF2R knockdown cells (data not shown). Resistance to uPAR cleavage in M6P/IGF2R knockdown cells might also have important implications for the nature of uPA signaling in these cells. Using a cleavage-resistant mutant of uPAR Mazzieri *et al.* (2006) showed that reduced cleavage of uPAR favored epidermal growth factor

receptor phosphorylation upon addition of uPA to cells (Mazzieri *et al.*, 2006).

Together, tumor cells loosing M6P/IGF2R expression become deficient in negative feedback regulation of the Plg activation system via uPAR cleavage resulting in enhanced invasive potential. We propose that the regulation of uPAR cleavage and  $\alpha$ V integrin expression by M6P/IGF2R could explain its potential role as a metastasis suppressor. Observations in clinical and experimental studies support this view. For example, the M6P/IGF2R expression was found decreased in invasive carcinomas relative to adjacent normal tissue and high-grade ductal carcinomas *in situ* in a breast cancer study (Berthe *et al.*, 2003). Furthermore, the overexpression of M6P/IGF2R in breast cancer cells reduced their invasive potential through Matrigel (Lee *et al.*, 2003). Recently, it has been shown that M6P/IGF2R is down-regulated by the major tumor promoting factor SATB1 (Han *et al.*, 2008). It was also shown that the regulation of uPAR cleavage might influence tumor progression. For example, highly invasive follicular thyroid carcinoma cells expressed the intact form uPAR, whereas less aggressive papillary carcinoma cells as well as benign thyroid tumor cells and nonneoplastic cells expressed large amounts of cleaved uPAR (Ragno *et al.*, 1998). We conclude that under *in vivo* conditions with high uPA/uPAR levels present, the M6P/IGF2R status of tumor cells might predict the invasive potential of these cells.

## ACKNOWLEDGMENTS

We are grateful to Eva Steinhuber for technical assistance. We acknowledge E. Wagner for the M6P/IGF2R-negative mouse fibroblasts, P. Petzelbauer for the human melanoma cell line IGR37, and V. Magdolen for the ovarian epithelial tumor cell line OVMZ-6. We thank V. Hořejší for mAbs MEM-238 and MEM-240 against M6P/IGF2R and MEM-101A against  $\beta$ 1 integrin, U. Weidle for mAbs C8 and H2 against uPAR, S. Stewart for the lentiviral vector pLKOpuo1, and D. Trono for the second generation lentiviral vector plasmids. This work was supported by the Austrian Science Fund (grant P19014-B13 and Program Project Grant SFBF005), grants from the Science and Technology Assistance Agency (APVT-51-026204), the Slovak Grant Agency VEGA (2/5119/25), the Bilateral Cooperation Slovakia-Austria (SK-11-AUT-9), the Competence Centre for Biomolecular Therapeutics (BMT) and the GEN-AU program of the Austrian Federal Ministry of Science and Research.

## REFERENCES

Arap, W., and Huang, H. J. (1999). Expression of Integrin Transcripts in Human Cancer Cells, Totowa, NJ: Humana Press.

Beaufort, N., Leduc, D., Rousselle, J. C., Namane, A., Chignard, M., and Pidard, D. (2004). Plasmin cleaves the juxtamembrane domain and releases truncated species of the urokinase receptor (CD87) from human bronchial epithelial cells. *FEBS Lett.* 574, 89–94.

Behrendt, N., Ploug, M., Patthy, L., Houen, G., Blasi, F., and Dano, K. (1991). The ligand-binding domain of the cell surface receptor for urokinase-type plasminogen activator. *J. Biol. Chem.* 266, 7842–7847.

Bernstein, A. M., Twining, S. S., Warejcka, D. J., Tall, E., and Masur, S. K. (2007). Urokinase receptor cleavage: a crucial step in fibroblast-to-myofibroblast differentiation. *Mol. Biol. Cell* 18, 2716–2727.

Berthe, M. L., Esslimani Sahla, M., Roger, P., Gleizes, M., Lemamy, G. J., Brouillet, J. P., and Rochefort, H. (2003). Mannose-6-phosphate/insulin-like growth factor-II receptor expression levels during the progression from normal human mammary tissue to invasive breast carcinomas. *Eur. J. Cancer* 39, 635–642.

Chen, J., Baskerville, C., Han, Q., Pan, Z. K., and Huang, S. (2001).  $\alpha$ (v) Integrin, p38 mitogen-activated protein kinase, and urokinase plasminogen activator are functionally linked in invasive breast cancer cells. *J. Biol. Chem.* 276, 47901–47905.

Cunningham, O., Andolfo, A., Santovito, M. L., Iuzzolino, L., Blasi, F., and Sidenius, N. (2003). Dimerization controls the lipid raft partitioning of uPAR/CD87 and regulates its biological functions. *EMBO J.* 22, 5994–6003.

Dano, K., Behrendt, N., Hoyer-Hansen, G., Johnsen, M., Lund, L. R., Ploug, M., and Romer, J. (2005). Plasminogen activation and cancer. *Thromb. Haemost.* 93, 676–681.

Dass, K., Ahmad, A., Azmi, A. S., Sarkar, S. H., and Sarkar, F. H. (2008). Evolving role of uPA/uPAR system in human cancers. *Cancer Treat. Rev.* 34, 122–136.

Dennis, P. A., and Rifkin, D. B. (1991). Cellular activation of latent transforming growth factor beta requires binding to the cation-independent mannose 6-phosphate/insulin-like growth factor type II receptor. *Proc. Natl. Acad. Sci. USA* 88, 580–584.

Ellis, V., Whawell, S. A., Werner, F., and Deadman, J. J. (1999). Assembly of urokinase receptor-mediated plasminogen activation complexes involves direct, non-active-site interactions between urokinase and plasminogen. *Biochemistry* 38, 651–659.

Felding-Habermann, B., Fransvea, E., O'Toole, T. E., Manzuk, L., Faha, B., and Hensler, M. (2002). Involvement of tumor cell integrin alpha v beta 3 in hematogenous metastasis of human melanoma cells. *Clin. Exp. Metastasis* 19, 427–436.

Felding-Habermann, B. *et al.* (2001). Integrin activation controls metastasis in human breast cancer. *Proc. Natl. Acad. Sci. USA* 98, 1853–1858.

Ghosh, P., Dahms, N. M., and Kornfeld, S. (2003). Mannose 6-phosphate receptors: new twists in the tale. *Nat. Rev. Mol. Cell Biol.* 4, 202–212.

Godar, S., Horejsi, V., Weidle, U. H., Binder, B. R., Hansmann, C., and Stockinger, H. (1999). M6P/IGFII-receptor complexes urokinase receptor and plasminogen for activation of transforming growth factor-beta1. *Eur. J. Immunol.* 29, 1004–1013.

Gruber, F. *et al.* (2003). Direct binding of Nur77/NAK-1 to the plasminogen activator inhibitor 1 (PAI-1) promoter regulates TNF alpha-induced PAI-1 expression. *Blood* 101, 3042–3048.

Guvakova, M. A. (2007). Insulin-like growth factors control cell migration in health and disease. *Int. J. Biochem. Cell Biol.* 39, 890–909.

Han, H. J., Russo, J., Kohwi, Y., and Kohwi-Shigematsu, T. (2008). SATB1 reprogrammes gene expression to promote breast tumour growth and metastasis. *Nature* 452, 187–193.

Hebert, E. (2006). Mannose-6-phosphate/insulin-like growth factor II receptor expression and tumor development. *Biosci. Rep.* 26, 7–17.

Hoyer-Hansen, G., Behrendt, N., Ploug, M., Dano, K., and Preissner, K. T. (1997). The intact urokinase receptor is required for efficient vitronectin binding: receptor cleavage prevents ligand interaction. *FEBS Lett.* 420, 79–85.

Hoyer-Hansen, G., Ronne, E., Solberg, H., Behrendt, N., Ploug, M., Lund, L. R., Ellis, V., and Dano, K. (1992). Urokinase plasminogen activator cleaves its cell surface receptor releasing the ligand-binding domain. *J. Biol. Chem.* 267, 18224–18229.

Kang, J. X., Li, Y., and Leaf, A. (1997). Mannose-6-phosphate/insulin-like growth factor-II receptor is a receptor for retinoic acid. *Proc. Natl. Acad. Sci. USA* 94, 13671–13676.

Kasper, D., Dittmer, F., von Figura, K., and Pohlmann, R. (1996). Neither type of mannose 6-phosphate receptor is sufficient for targeting of lysosomal enzymes along intracellular routes. *J. Cell Biol.* 134, 615–623.

Kobayashi, H., Schmitt, M., Goretzki, L., Chucholowski, N., Calvete, J., Kramer, M., Gunzler, W. A., Janicke, F., and Graeff, H. (1991). Cathepsin B efficiently activates the soluble and the tumor cell receptor-bound form of the proenzyme urokinase-type plasminogen activator (Pro-uPA). *J. Biol. Chem.* 266, 5147–5152.

Koshelnick, Y., Ehart, M., Hufnagel, P., Heinrich, P. C., and Binder, B. R. (1997). Urokinase receptor is associated with the components of the JAK1/STAT1 signaling pathway and leads to activation of this pathway upon receptor clustering in the human kidney epithelial tumor cell line TCL-598. *J. Biol. Chem.* 272, 28563–28567.

Kreiling, J. L., Byrd, J. C., Deisz, R. J., Mizukami, I. F., Todd, R. F., 3rd, and MacDonald, R. G. (2003). Binding of urokinase-type plasminogen activator receptor (uPAR) to the mannose 6-phosphate/insulin-like growth factor II receptor: contrasting interactions of full-length and soluble forms of uPAR. *J. Biol. Chem.* 278, 20628–20637.

Lee, J. S., Weiss, J., Martin, J. L., and Scott, C. D. (2003). Increased expression of the mannose 6-phosphate/insulin-like growth factor-II receptor in breast cancer cells alters tumorigenic properties *in vitro* and *in vivo*. *Int. J. Cancer* 107, 564–570.

Leivonen, S. K., and Kahari, V. M. (2007). Transforming growth factor-beta signaling in cancer invasion and metastasis. *Int. J. Cancer* 121, 2119–2124.

Leksa, V., Godar, S., Cebebauer, M., Hilgert, I., Breuss, J., Weidle, U. H., Horejsi, V., Binder, B. R., and Stockinger, H. (2002). The N terminus of

- mannose 6-phosphate/insulin-like growth factor 2 receptor in regulation of fibrinolysis and cell migration. *J. Biol. Chem.* 277, 40575–40582.
- Leksa, V. *et al.* (2005). TGF- $\beta$ -induced apoptosis in endothelial cells mediated by M6P/IGFII-R and mini-plasminogen. *J. Cell Sci.* 118, 4577–4586.
- Lorenzo, K., Ton, P., Clark, J. L., Coulibaly, S., and Mach, L. (2000). Invasive properties of murine squamous carcinoma cells: secretion of matrix-degrading cathepsins is attributable to a deficiency in the mannose 6-phosphate/insulin-like growth factor II receptor. *Cancer Res.* 60, 4070–4076.
- Lutz, V., Reuning, U., Kruger, A., Luther, T., von Steinburg, S. P., Graeff, H., Schmitt, M., Wilhelm, O. G., and Magdolen, V. (2001). High level synthesis of recombinant soluble urokinase receptor (CD87) by ovarian cancer cells reduces intraperitoneal tumor growth and spread in nude mice. *Biol. Chem.* 382, 789–798.
- MacDonald, R. G., and Byrd, J. C. (2003). The insulin-like growth factor II/mannose 6-phosphate receptor: implications for IGF action in breast cancer. *Breast Dis.* 17, 61–72.
- Madsen, C. D., Ferraris, G. M., Andolfo, A., Cunningham, O., and Sidenius, N. (2007). uPAR-induced cell adhesion and migration: vitronectin provides the key. *J. Cell Biol.* 177, 927–939.
- Madsen, C. D., and Sidenius, N. (2008). The interaction between urokinase receptor and vitronectin in cell adhesion and signalling. *Eur. J. Cell Biol.* 87, 617–629.
- Mazar, A. P., Henkin, J., and Goldfarb, R. H. (1999). The urokinase plasminogen activator system in cancer: implications for tumor angiogenesis and metastasis. *Angiogenesis* 3, 15–32.
- Mazzieri, R., D'Alessio, S., Kenmoe, R. K., Ossowski, L., and Blasi, F. (2006). An uncleavable uPAR mutant allows dissection of signaling pathways in uPA-dependent cell migration. *Mol. Biol. Cell* 17, 367–378.
- Montuori, N., Carriero, M. V., Salzano, S., Rossi, G., and Ragno, P. (2002). The cleavage of the urokinase receptor regulates its multiple functions. *J. Biol. Chem.* 277, 46932–46939.
- Montuori, N., Visconte, V., Rossi, G., and Ragno, P. (2005). Soluble and cleaved forms of the urokinase-receptor: degradation products or active molecules? *Thromb. Haemost.* 93, 192–198.
- Motyka, B. *et al.* (2000). Mannose 6-phosphate/insulin-like growth factor II receptor is a death receptor for granzyme B during cytotoxic T cell-induced apoptosis. *Cell* 103, 491–500.
- Naldini, L., Blomer, U., Gallay, P., Ory, D., Mulligan, R., Gage, F. H., Verma, I. M., and Trono, D. (1996). In vivo gene delivery and stable transduction of nondividing cells by a lentiviral vector. *Science* 272, 263–267.
- Nykjaer, A., Christensen, E. I., Vorum, H., Hager, H., Petersen, C. M., Roigaard, H., Min, H. Y., Vilhardt, F., Moller, L. B., Kornfeld, S., and Gliemann, J. (1998). Mannose 6-phosphate/insulin-like growth factor-II receptor targets the urokinase receptor to lysosomes via a novel binding interaction. *J. Cell Biol.* 141, 815–828.
- Nykjaer, A., Conese, M., Christensen, E. I., Olson, D., Cremona, O., Gliemann, J., and Blasi, F. (1997). Recycling of the urokinase receptor upon internalization of the uPA:serpin complexes. *EMBO J.* 16, 2610–2620.
- Pilch, J., Habermann, R., and Felding-Habermann, B. (2002). Unique ability of integrin  $\alpha(v)\beta 3$  to support tumor cell arrest under dynamic flow conditions. *J. Biol. Chem.* 277, 21930–21938.
- Prager, G. W., Breuss, J. M., Steurer, S., Olcaydu, D., Mihaly, J., Brunner, P. M., Stockinger, H., and Binder, B. R. (2004). Vascular endothelial growth factor receptor-2-induced initial endothelial cell migration depends on the presence of the urokinase receptor. *Circ. Res.* 94, 1562–1570.
- Ragno, P. (2006). The urokinase receptor: a ligand or a receptor? Story of a sociable molecule. *Cell Mol. Life Sci.* 63, 1028–1037.
- Ragno, P., Montuori, N., Covelli, B., Hoyer-Hansen, G., and Rossi, G. (1998). Differential expression of a truncated form of the urokinase-type plasminogen-activator receptor in normal and tumor thyroid cells. *Cancer Res.* 58, 1315–1319.
- Ravanko, K., Jarvinen, K., Helin, J., Kalkkinen, N., and Holttä, E. (2004). Cysteine cathepsins are central contributors of invasion by cultured adenosylmethionine decarboxylase-transformed rodent fibroblasts. *Cancer Res.* 64, 8831–8838.
- Resnati, M., Pallavicini, L., Wang, J. M., Oppenheim, J., Serhan, C. N., Romano, M., and Blasi, F. (2002). The fibrinolytic receptor for urokinase activates the G protein-coupled chemotactic receptor FPRL1/LXA4R. *Proc. Natl. Acad. Sci. USA* 99, 1359–1364.
- Rolli, M., Fransvea, E., Pilch, J., Saven, A., and Felding-Habermann, B. (2003). Cysteine cathepsins cooperate with metalloproteinase MMP-9 in regulating migration of metastatic breast cancer cells. *Proc. Natl. Acad. Sci. USA* 100, 9482–9487.
- Samani, A. A., Yakar, S., LeRoith, D., and Brodt, P. (2007). The role of the IGF system in cancer growth and metastasis: overview and recent insights. *Endocr. Rev.* 28, 20–47.
- Scott, C. D., and Firth, S. M. (2004). The role of the M6P/IGF-II receptor in cancer: tumor suppression or garbage disposal? *Horm. Metab. Res.* 36, 261–271.
- Smith, H. W., Marra, P., and Marshall, C. J. (2008). uPAR promotes formation of the p130Cas-Crk complex to activate Rac through DOCK180. *J. Cell Biol.* 182, 777–790.
- Tarui, T. *et al.* (2006). Direct interaction of the kringle domain of urokinase-type plasminogen activator (uPA) and integrin  $\alpha v \beta 3$  induces signal transduction and enhances plasminogen activation. *Thromb. Haemost.* 95, 524–534.
- Tarui, T., Majumdar, M., Miles, L. A., Ruf, W., and Takada, Y. (2002). Plasmin-induced migration of endothelial cells. A potential target for the anti-angiogenic action of angiostatin. *J. Biol. Chem.* 277, 33564–33570.
- van den Hoff, M. J., Moorman, A. F., and Lamers, W. H. (1992). Electroporation in 'intracellular' buffer increases cell survival. *Nucleic Acids Res.* 20, 2902.
- Wei, C. *et al.* (2008). Modification of kidney barrier function by the urokinase receptor. *Nat. Med.* 14, 55–63.